2-13-2010

The Effect of ACE Inhibition on the Pulmonary Vasculature in Combined Models of Chronic Hypoxia and Pulmonary Arterial Banding in Sprague Dawley Rats

Shanelle Clarke
Medical College of Wisconsin

Shelley Baumgardt
Zablocki Veteran Affairs Medical Center

Robert C. Molthen
Marquette University, robert.molthen@marquette.edu

Published version. Published as part of the proceedings of the conference, *Medical Imaging 2010: Biomedical Applications in Molecular, Structural, and Functional Imaging*, 2010. DOI.

The effect of ACE inhibition on the pulmonary vasculature in combined models of chronic hypoxia and pulmonary arterial banding in sprague dawley rats

Shanelle Clarke[1], Shelley Baumgardt[4], Robert Molthen[2,3,4]

[1] Department of Pediatrics, Division of Critical Care, Medical College of Wisconsin, Milwaukee, WI, USA 53226

[2] Department of Medicine, Division of Critical Care, Medical College of Wisconsin, Milwaukee, WI, USA 53226

[3] Marquette University, Milwaukee, WI 53201

[4] Zablocki Veteran Affairs Medial Center, Milwaukee, WI 53201

ABSTRACT

Microfocal CT was used to image the pulmonary arterial (PA) tree in rodent models of pulmonary hypertension (PH). CT images were used to measure the arterial tree diameter along the main arterial trunk at several hydrostatic intravascular pressures and calculate distensibility. High-resolution planar angiographic imaging was also used to examine distal PA microstructure. Data on pulmonary artery tree morphology improves our understanding of vascular remodeling and response to treatments. Angiotensin II (ATII) has been identified as a mediator of vasoconstriction and proliferative mitotic function. ATII has been shown to promote vascular smooth muscle cell hypertrophy and hyperplasia as well as stimulate synthesis of extracellular matrix proteins. Available ATII is targeted through angiotensin converting enzyme inhibitors (ACEIs), a method that has been used in animal models of PH to attenuate vascular remodeling and decrease pulmonary vascular resistance. In this study, we used rat models of chronic hypoxia to induce PH combined with partial left pulmonary artery occlusion (arterial banding, PLPAO) to evaluate effects of the ACEI, captopril, on pulmonary vascular hemodynamic and morphology. Male Sprague Dawley rats were placed in hypoxia (FiO2 0.1), with one group having underwent PLPAO three days prior to the chronic hypoxia. After the twenty-first day of hypoxia exposure, treatment was started with captopril (20 mg/kg/day) for an additional twenty-one days. At the endpoint, lungs were excised and isolated to examine: pulmonary vascular resistance, ACE activity, pulmonary vessel morphology and biomechanics. Hematocrit and RV/LV+septum ratio was also measured. CT planar images showed less vessel dropout in rats treated with captopril versus the non-treatment lungs. Distensibility data shows no change in rats treated with captopril in both chronic hypoxia (CH) and CH with PLPAO (CH+PLPAO) models. Hemodynamic measurements also show no change in the pulmonary vascular resistance with captopril treatment in both CH and CH+PLPAO.

Keywords: angiotensin, ACEI, microfocal CT, pulmonary hypertension, distensibility, planar angiogram, rat model

1. INTRODUCTION

Pediatric patients with congenital heart disease, specifically with left to right shunts, are known to develop pulmonary hypertension (PH). Repair of the shunt at a young age decreases the risk of developing pulmonary hypertension but there are some patients that continue to develop elevated pulmonary vascular resistance[31]. Some of these children have other co-morbidities that predispose them to PH, such as prematurity or chronic lung disease. The pathologic changes that occur in PH secondary to congenital heart disease are similar to changes that occur in idiopathic PH. Pathologically, there is hypertrophy and hyperplasia of the media and, in some cases, development of plexiform lesions[23,33]. In rat models of PH with prolonged vasoconstriction caused by chronic hypoxic exposure there is stimulation of vascular remodeling and extension of vascular smooth muscle cells in to more distal previously non-muscular arteries[2,6,25,33].

Medical Imaging 2010: Biomedical Applications in Molecular, Structural, and Functional Imaging, edited by Robert C. Molthen, John B. Weaver, Proc. of SPIE Vol. 7626, 762614 · © 2010 SPIE
CCC code: 1605-7422/10/$18 · doi: 10.1117/12.846387

Though the causes of PH are not fully known, hypoxia, inflammation, and endothelial injury are all known stimuli for the vasoconstriction and vascular remodeling that occurs in PH. Vasoconstriction occurs due to an imbalance between vasoconstrictor and vasodilator mediators in the pulmonary vascular bed[10]. There is a decrease in vasodilators, nitric oxide and prostocyclin, and an increase in vasoconstrictors, endothelin-1, and thromboxane A_2. Prolonged vasoconstriction leads to vascular remodeling, which is mostly irreversible, as we know it. Current therapies often aim to change the balance between vasoactive mediators such as endothelin-1 antagonists, prostocyclin, and nitric oxide. Although these therapies slow the progression of the disease, they do not reverse it. Some studies have looked at the mediators involved in vascular remodeling[11,16,22,34] and the effects of modulating mediators to attenuate vascular remodeling. One such mediator is angiotensin II.

Angiotensin II (ATII) has many effects on the vasculature. The two main ATII mechanisms involve vasoconstrictive and mitogenic activity. ATII is created by an enzymatic conversion of angiotensin I by angiotensin converting enzyme (ACE), which is primarily found in the lung. ACE has been shown to reduce vasodilatation by inactivation of bradykinin[12]. ATII promotes smooth muscle cell hypertrophy, hyperplasia and migration to the non-muscular pulmonary vasculature[4,21]. Expression of ACE has been shown to increase after exposure to CH[20]. Angiotensin converting enzyme inhibitors (ACEIs) decrease available ATII. Studies have been done to examine the effect of ACEIs on the development of increased pulmonary vascular resistance. ACEIs modulate vascular remodeling and decreases pulmonary vascular resistance that occurs in chronic hypoxia[5,12,22,26]. However, previous studies have started ACEI treatment prior to or at the same time the stimulus causing PH and vascular remodeling (i.e. hypoxia or monocrotaline) was applied. This is a preventative model of PH and cannot be used to infer treatment benefits in patients with established pulmonary hypertension. Studies that have started therapy with an ACEI after establishment of pulmonary hypertension have mixed results, with some showing a beneficial decrease in pulmonary vascular resistance and others showing no benefit[3,15,22].

Along with the distal extension of smooth muscle cells into non-muscular arteries and hyperplasia of the arterial media layer, studies have shown evidence of rarefactions and loss of arterioles[6,18,24], which is thought to be an important component of PH. Other evidence of angiogenesis in the systemic vasculature in rats exposed to CH[8,9,31] may not be reflective of what is occurring in the pulmonary vascular bed, although recent study by Howell et al. showed that rat exposed to CH have increased blood vessel volume and length as well as increase capillary surface area[9]. Results from imaging experiments in this study provide further evidence of vessel rarefaction with chronic hypoxia induced PH.

2. STUDY DESIGN

This study was designed to examine the effect of an orally ingested angiotensin converting enzyme inhibitor (captopril) on the pulmonary vasculature in rats with established pulmonary hypertension. Toward this goal we utilized male sprague dawley rats weighing 250-300gm in two models of PH, one of chronic hypoxic (CH) exposure and a second of CH exposure after partial left pulmonary artery banding. The Institutional Animal Care and Use Committee of the Zablocki VA Medical Center approved all protocols and procedures. In both the CH group (N = 8) and the CH + banding group (N = 8), half of the rats received treatment with captopril after the first 21-days of exposure. A control group had partial left pulmonary artery banding, was kept in normoxia, and did not receive captopril (N = 4).

2.1 Hypoxia

Hypoxia chambers had a FiO_2 of 0.1, which was achieved by blending room air with N_2. The FiO_2 was monitored and maintained for constant FiO_2 at least twice daily. The rats were kept in the chamber except for food, water, weighing, and bedding and cage changes twice weekly. These maintenance routines took under 30 minutes to complete and all rats, except for the normoxics, were kept in CH for a total of 42-days.

2.2 Partial Left Pulmonary Artery Occlusion

Some rats underwent surgical partial left pulmonary artery occlusion (PLPAO) 3 days prior to placement in hypoxia chambers (N = 8). The rats were anesthetized with a subcutaneous injection of ketamine (75mg/kg) and dormitor (0.5mg/kg). They were weighed and, once a sufficient plane of anesthesia was obtained, intubated with a 14 gauge angiocath, placed on a ventilator (*Harvard Apparatus model Inspira asv model# 55-7059*) and ventilated with a peak pressure of 32 cmH_2O, peep of 7 cmH_2O, and an initial rate of 72 breaths/minute. The chest was opened at the fourth intercostal space and the left lung deflated. The left pulmonary artery was identified and dissected away from the airway

and partially occluded using a loop of nylon suture around the artery. The lung was re-inflated by using sigh breaths of 40 cmH_20 peak pressure. When the lung was fully re-inflated the chest was closed in two layers using nylon suture. During skin closure each rat was given 10mg/kg of Baytril subcutaneously and Antisedan (1mg/kg) by intraperitoneal injection. When the rat began to spontaneously breath at a regular rate, the endotracheal tube was removed. They were placed on a heating pad, given 2ml of normal saline subcutaneously and 0.1-0.5mg of Buprenex subcutaneously and were allowed to recover.

2.3 Captopril

The rats that received treatment with an ACEI were provided captopril (20mg/kg/day) in their drinking water, starting the 22nd day of CH exposure.

2.4 Endpoint Studies

Endpoint studies (day 42) included measurements of hematocrit, body weight, RV/LV+septum ratio, FAPGG, dry lung weight, hemodynamics, and micro-CT imaging to measure distensibility, diameter, and the length of the main pulmonary trunk.

Each rat was anesthetized with sodium pentobarbital (40 mg/kg ip) and a midline sternotomy was performed. The rat was heparinized (200 IU/kg) by right ventricular injection, and a blood sample was removed for hematocrit determination. The trachea and pulmonary artery were cannulated, and the heart was excised for right ventricular free wall and left ventricle plus septum weight determination. The lung was ventilated with a 15% O_2, 6 % CO_2 in N_2 gas mixture, 3 mmHg end expiratory pressure and 8 mmHg end inspiratory pressure. The lung was subjected to 2 or 3 brief peak inspiratory episodes of 12- 15 mmHg to eliminate any atelectasis that might have occurred during the excision. The lung was rinsed free of blood and perfused with a 37°c physiological salt solution containing 5% bovine serum albumin.

2.4.1 Hematocrit, RV/LV + septum Ratio, and Hemodynamics

Blood drawn from the heart was centrifuged at 30,000 rpm for at least 2 minutes and the ratio of packed cells to plasma was used to determine hematocrit. Two samples were prepared from each rat and the average value reported. The heart was excised and the right ventricle was dissected from the left ventricle and ventricular septum. Each was weighed and the ratio was used to indicate right ventricular hypertrophy (RVH). A recirculation circuit was created with the excised lung with the physiologic saline solution with 5% bovine serum albumin. Hemodynamic studies were performed by measuring the pulmonary artery pressure at several flow rates from 0 to 40ml/min while maintaining a constant airway pressure of 6 mmHg. The flow was normalized to rat body weight for graphical analysis.

2.4.2 FAPGG

N-[3-(2-furyl)-acrylol]-L-phenyl-alanyglyclglycine (FAPGG) is an ACE substrate used to determine the activity of ACE. FAPGG is hydrolyzed to FAP and there is a resultant decrease in absorbance at 340nm[10]. FAPGG is perfused through the lung for 50 sec then samples of the effluent are obtained at 55 and 60 sec for the full lung. The effluent samples were placed in a spectrometer and the absorbance measured and used as and indicator of the binding activity of ACE. ACE activity is presented as means surface area product (MSAP).

2.4.3 Microfocal Angiography and CT Imaging and Analysis

The lung was immediately placed in the imaging chamber and ventilated with the gas mixture listed above. An atmospheric reservoir of perfluorooctyl bromide (PFOB), an X-ray contrast agent, was connected to the pulmonary artery cannula via clamped 1/8 inch ID Tygon tubing. The tubing was unclamped and the physiologic saline solution in the lung was then replaced by PFOB. Because, PFOB does not pass through the capillary bed, it only fills the pulmonary arterial tree and intravascular pressures can be maintained hydrostatically. Accounting for the density of the PFOB, intravascular pressure was determined by measuring the difference between the height of the surface of PFOB in the reservoir and the center of the lung. The arteries were conditioned by cycling the intravascular pressure from 0 to 30 mmHg several times. Ventilation was halted during imaging, airway pressure was again maintained constant at 6 mmHg. The arterial pressure was set to 30 mmHg, and the lungs were rotated in the x-ray beam of a custom built microfocal

imaging system[14,18] at 1° increments to obtain 360 planar images. The pressure was lowered successively to 21, 12, and 6 mmHg, with complete CT scans obtained at each pressure (see Figure 4). Each scan took approximately 3 minutes. The lungs were then translated toward the X-ray source and high-magnification planar images of each lung lobe were obtained at each intravascular pressure.

Arterial distensibility was measured using previously published methods[30]. Briefly, isotropic CT volumes of the isolated lungs were obtained at each of the four intravascular pressures. *A Visualization Workshop* (AVW, Analyze® *Biomedical Imaging Resource (BIR) at the Mayo Clinic*[27,28,29] was used to segment and map the main pulmonary trunk. Consecutive 2-dimensional orthogonal planes along the main pulmonary trunk were then fit to a modified Guassian function, by a process of two-stage numeric optimization. The vessel diameter estimation was performed using a technique of multidimensional, constrained non-linear least squares fitting and a variant of the Levenberg-Marquardt least squares minimization implemented by Manolis Lourakis[17] was used under the terms of the GNU General Public License[3]. To estimate arterial distensibility, the data were fit to a morphometric model of the pulmonary arterial tree, which incorporates a well-accepted model of pulmonary arterial distensibility using the unconstrained multivariable non-linear optimization function 'fminunc' in the Matlab optimization toolbox (MathWorks, Natick, MA).

3. RESULTS

Statisticsal significance was determined by performing paired t-test and a one way ANOVA and all graphs plot mean values with standard error bars. CH significantly increased the hematocrit, however, there was no significant difference in hematocrit levels in rats treated with captopril and those provided only water. Hematocrit in CH and CH+PLPAO groups was not significantly different with and without captopril treatment. However, there is a statistically significant difference between the hematocrit of the PLPAO normoxic group and all the other groups, $p<0.025$. Hypoxia is a significant stimulus for red blood cell production and captopril treatment did not alter the stimulus effect.

ACE activity was inhibited in the rats that were treated with captorpil, confirmed by the decreased mean surface area product in treated rats. The ACE activity was not significantly different in the CH, CH+PLPAO, and PLPAO normoxic rats that did not receive captopril treatment.

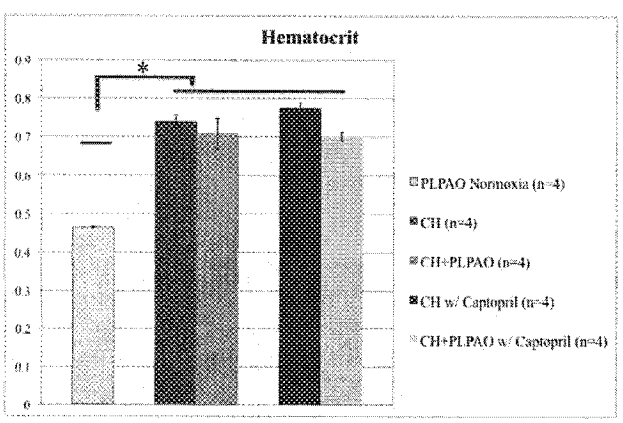

Figure 1. Hematocrit
*Bars represent the mean value of hematocrit in CH+PLPAO, CH+PLPAO w/ captopril, CH, CH w/ captopril and PLPAO Normoxia. Error bars are ± standard error. *p < 0.025*

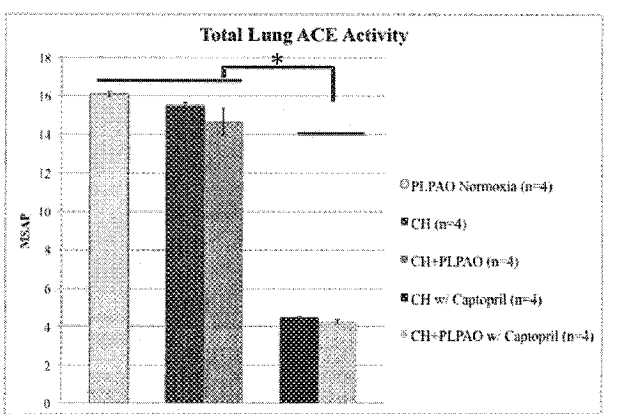

Figure 2. Total Lung ACE Activity
*Bars represent the mean value of total lung ACE activity as mean surface area product measured in isolated lungs from CH+PLPAO, CH+PLPAO w/ captopril, CH, CH w/ captopril, and PLPAO Normoxia rats. Error bars are ± standard error. *p < 0.001*

Rats in the CH and CH+PLPAO groups (whether treated or not) had significantly increased RVH compared to PLPAO normoxic rats as seen in Figure 3 with a $p<0.001$. Although there was a tendency toward a further increase in RVH, the RV/ LV + Septum mass ratio was not statistically significantly different between the CH and CH+ PLPAO groups. This is an indicator that the in vivo pulmonary vascular resistance likely remained elevated in rats treated with captopril, pulmonary pressure versus flow data below supports this.

The lung hemodynamic data is presented in Figure 4. The main pulmonary artery pressures measured at the various flow rates are graphed with flow normalized to body weight. The PA pressure is significantly increased in the CH and CH+PLPAO treatment and non-treatment groups compared to normoxia, as expected. However, Figure 4 shows no significance difference in pulmonary vascular resistance of any of the CH animals, whether with or without PLPAO or with or without captopril. Treatment with captopril did not lower the pulmonary vascular resistance and the pressure obtained for a given flow remains elevated to a comparable level in the treatment groups.

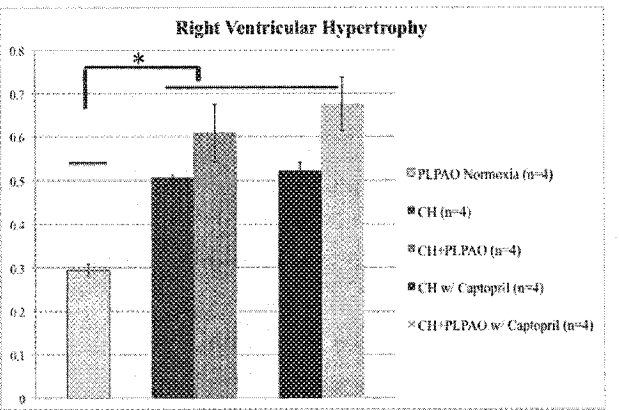

Figure 3. Right Ventricular Hypertrophy

*Right Ventricular Hypertrophy is expressed as the RV/LV+septum ratio. Bars represent the mean values in CH+PLPAO, CH+PLPAO w/ captopril, CH, CH w/ captopril, and PLPAO normoxia. Error bars are ± standard error. *p<0.001*

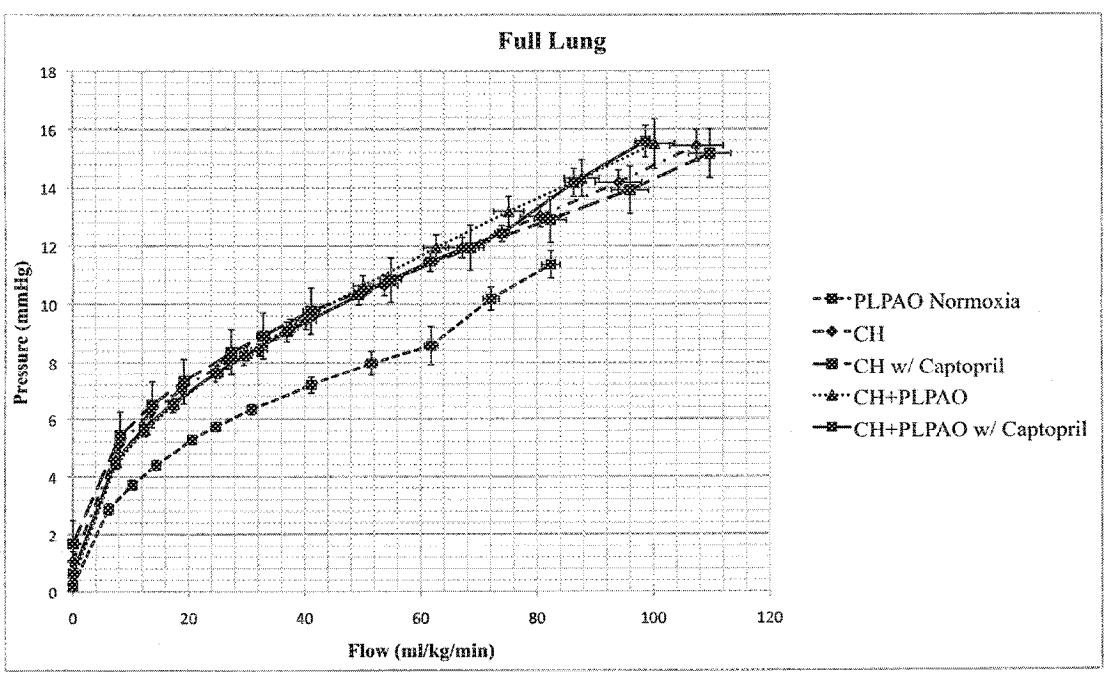

Figure 4. Hemodynamics of Full Lung

Flow is normalized to rat body weight and is in units of ml/kg/min and pressure is in mmHg. Error bars are ± standard error

Planar angiograms of the contrast filled arteries from selected lungs from each group are presented in Figures 5 and 6. These images were obtained from the highest (30 mmHg) and lowest (6 mmHg) intravascular pressures measured.

The images of both treated and non-treated groups show fewer peripheral vessels than the PLPAO rats kept in normoxia. However, the rats treated with captopril had less vessel dropout than those that did not receive treatment. This pattern of vessel dropout was more apparent at the higher intravascular pressure 30 mmHg (Figure 6). The images also show slight apparent parenchymal edema in the CH and CH+PLPAO groups compared to the PLPAO normoxic group. The edema appeared more exaggerated in the lungs of rats treated with captopril compared to untreated.

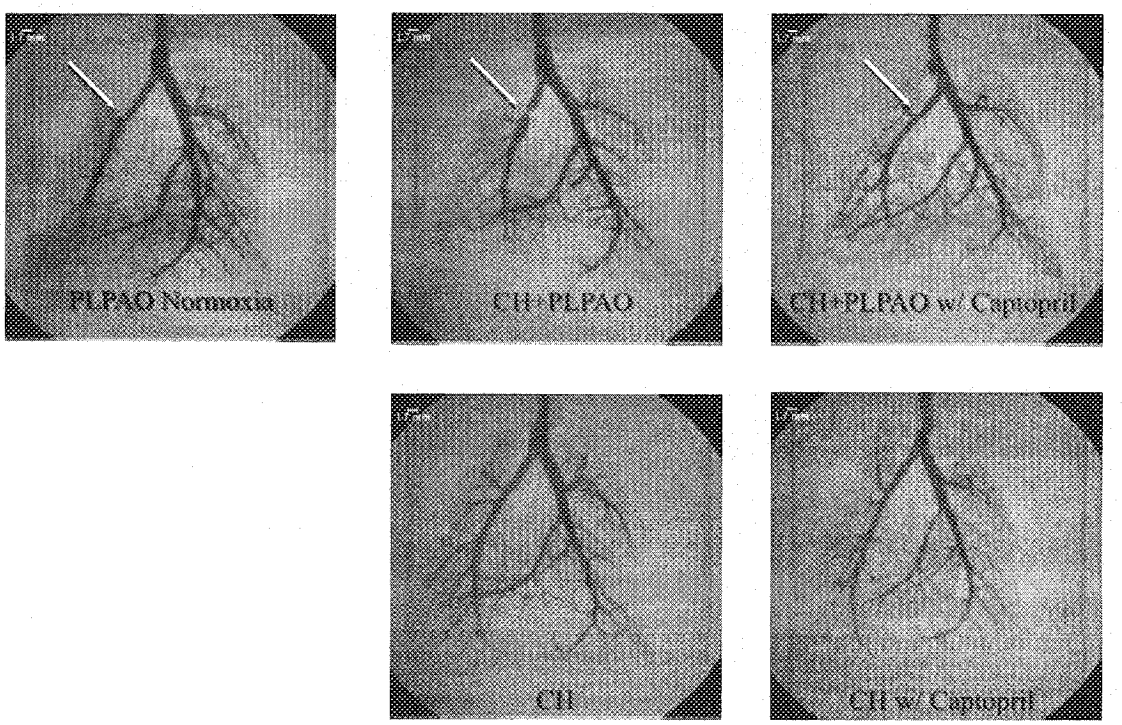

Figure 5. Low-Magnification Images of Full Lung at 6 mmHg
Scale in upper right represents 1.7mm. Arrow indicates area of PLPAO

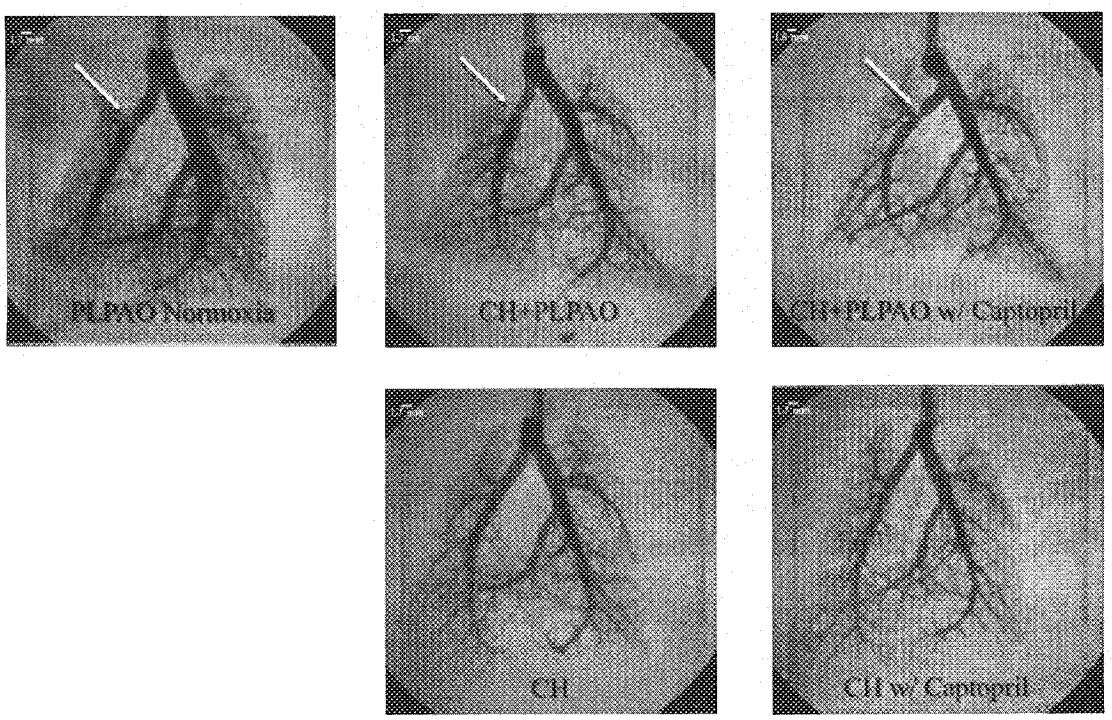

Figure 6. Low-Magnification Images of Full Lung at 30 mmHg
Scale in upper right represents 1.7mm. Arrow indicates area of PLPAO

High-magnification planar angiograms of the distal right arterial tree, presented in Figures 7 and 8, reveal more evidence of the vessel dropout in both CH and CH+PLPAO groups compared to the normoxic PLPAO rats. Again, the images suggest that there is less parenchymal vessel dropout in the treatment groups, in particular rats with CH+PLPAO and captopril treatment. In general, there appeared to be less dropout in the CH+PLPAO rats compared to exposed to CH without the banding.

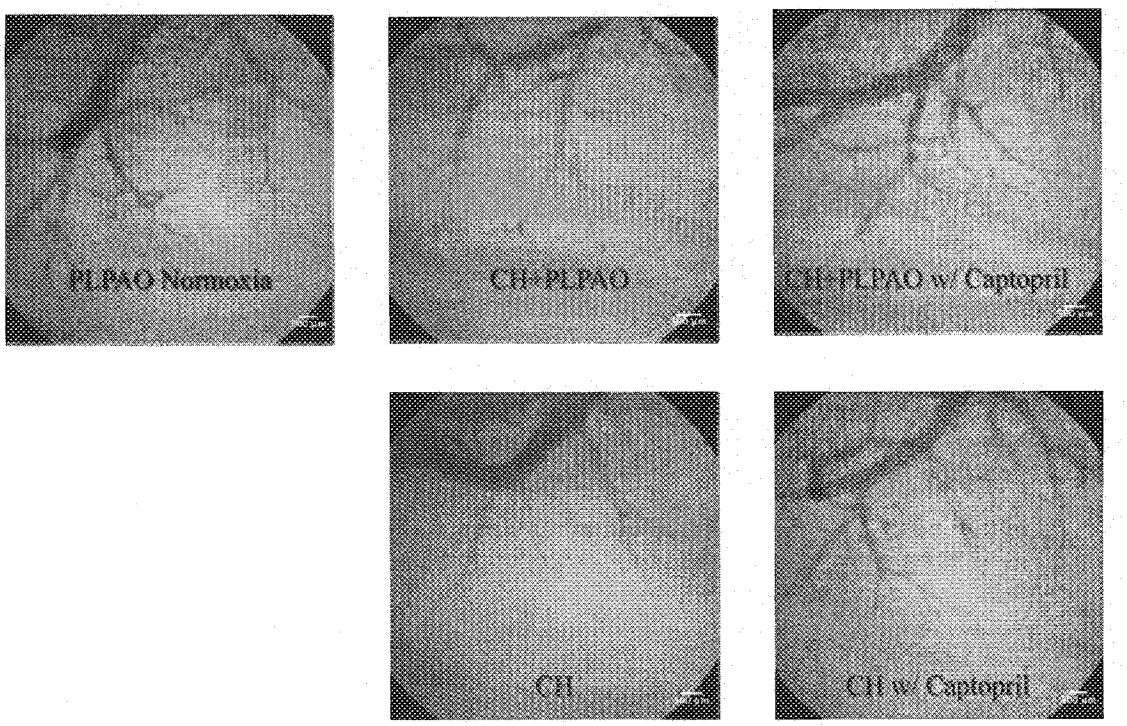

Figure 7. High Magnification of the Right Lung at 6 mmHg
Scale bar represents 500μm

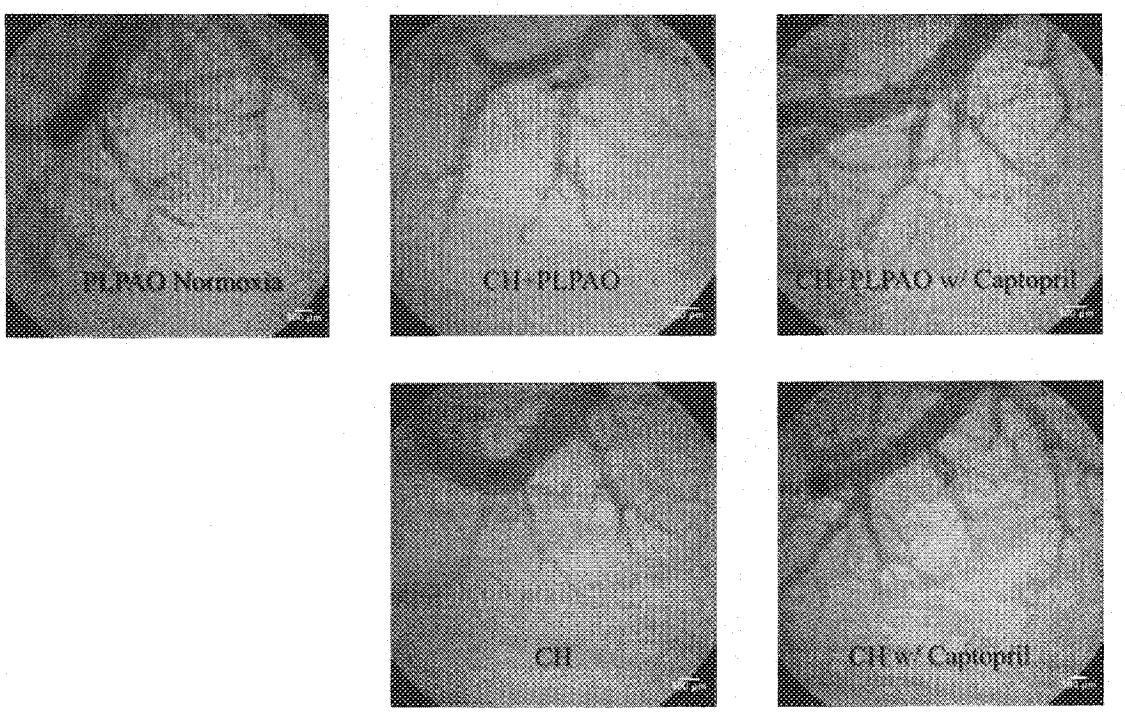

Figure 8. High Magnification of the Right Lung at 30 mmHg
Scale bar represents 500μm

Figure 9 shows data from the main right pulmonary arterial trunk measured in microfocal CT images for a selected lung. The graph presents vessel diameter versus the distance from the arterial inlet, at four intravascular pressures. The grey surface represents the fit to the morphological model[19] and the tilt of the surface along the pressure axis reflects the arterial distensibility.

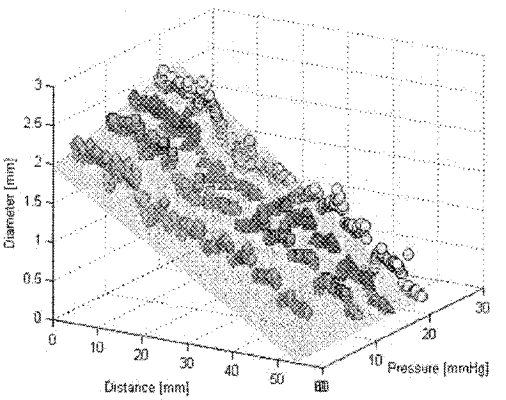

Figure 9. Principal pathway data for a selected lung

The morphologic model is given in by Eq. 1 below, where D(x,P) represents the vessel diameter, x is the distance from the inlet, P is the intravascular pressure, D(0,0) is the unstressed diameter of the inlet, α is a distensibility coefficient, *c* is a measure of the taper of the main trunk, and L_{tot} is the total length of the main trunk[19].

$$D(x,P) = D(0,0)(1+\alpha P)\left(1-\frac{x}{L_{tot}}\right)^{c} \quad \text{Eq. (1)}$$

Morphologic data is shown in Table 1. This data indicates distensibility (α) was unchanged by captopril treatment. The pulmonary artery inlet diameter,D(0,0), and the total length of the pulmonary trunk,L_{tot}, were not different between captopril treated and non-treated rats.

	CH *(n = 3)*	**CH w/ captopril** *(n = 2)*	**CH+PLPAO** *(n = 4)*	**CH+PLPAO w/ captopril** *(n = 4)*
No. Vessels Measured	445 ± 13	408 ± 1	409 ± 9	389 ± 10
D(0,0) (mm)	1.73 ± 0.19	1.75 ± 0.33	1.86 ± 0.14	1.806 ± 0.232
L_{tot} (mm)	55 ± 1	53 ± 1	53 ± 1	53 ± 1
α (1/mmHg)	0.017 ± 0.002	0.012 ± 0.0008	0.012 ± 0.003	0.017 ± 0.003

Table 1. Morphometric Data. No of vessel segments along the main pulmonary trunk used in the analysis, D(0,0) is the unstressed vessel diameter at the arterial trunk inlet, L_{tot} is the total length of the main trunk, and α is the arterial tree distensibility.

4. DISCUSSION

There are few studies evaluating the effect of ACEI on vascular remodeling in a rat model of established pulmonary hypertension[1,13,22]. Previous studies, in which PH is already established, have shown mixed hemodynamic changes with ACEI treatment. Nong et al. showed that treatment with ACEI (quinapril) in established PH did reduce the pulmonary artery pressure and degree of vascular remodeling[22], while Clozel et al. showed a decrease in pulmonary artery pressure and hematocrit with treatment with cilazapril[1]. Jeffery et al. showed mixed effects based on the dose of perindopril with higher doses causing a slight reduction in pulmonary artery pressures[13]. This study is unique in that we used CT imaging techniques to further interpret the hemodynamic data obtained. The CT images were used to quantify morphology and biomechanics in the pulmonary arterial tree. The planar images, in conjunction with the morphometric data, provide a picture of practically fixed distensibility between treatment and non-treatment groups with less vessel dropout peripherally in the treatment groups. The high-magnification planar angiograms indicate less vessel dropout in the treatment groups versus the non-treatment groups, which may be mitigation or a change in the evolution of vascular remodeling. This would suggest that there should be less elevation in the PVR of the rats treated with captopril. However, our hemodynamic and right ventricular hypertrophy data is contrary and shows no difference in PVR or RVH between treated and non-treated rats. The morphologic analysis shows no statistically significant differences in diameter, length, or distensibility between the rats that received captopril and those that did not. These results imply that although there are more arterial vessels present in the captopril treated lungs, the network of vessels present have a larger PVR. This increase in PVR could be, in part, explained by the increased secondary parenchymal edema present in the captopril treated rats. This would be especially the case in vivo given the high hematocrit levels seen in these animals[35]. The increase in parenchymal edema results in stiff and less compliant lungs, which may translate to the persistent elevation in PVR despite more peripheral vessels. Interestingly, L_{tot} was not was increased with captopril treatment. If anything, the CT data suggests the CH group tended to have a longer trunk length. These findings most likely indicate that any elongation is occurring in the larger vessel. Because our current analysis relies on detection of a single main trunk, evaluation of peripheral density is not adequately represented by L_{tot}.

The CH+PLPAO model was used to simulate the increased flow that is seen in pediatric patients with congenital heart disease. There is no statistically significant difference in the measured arterial distensibility between CH and CH+PLPAO with or without treatment, but the hemodynamics show a trend toward higher PA pressures in the CH+PLPAO groups as well as a trend toward a higher degree of RVH. This suggests that CH+PLPAO results in a higher in vivo PA pressure or there is hematopoietic or other signaling that results from the PLPAO banding. Increased flow and shear stress, causing more endothelial injury, may be a dependent factor that affects the condition of the right heart. This relationship would need to be further evaluated with additional studies.

CT angiography in models of lung disease in small animals described by Shingrani et al[30] and Molthen et al[18] is a relatively new method for assessing the pulmonary vascular tree. Imaging of the vascular bed allows for morphometric and biomechanical information to be obtained, which can then be used in conjunction with biochemical studies to further tailor therapies. Although captopril did not have a net beneficial effect on hemodynamics of the pulmonary vasculature in this study, ACEI treatment did affect the vascular morphology of the pulmonary arterial bed. This suggests that although captopril by itself may not provide a benefit to pulmonary hemodynamics, its use in altering the vessel morphology may be through combinational therapies.

5. REFERENCES

1. Clozel JP, Saunier C, Hartemann D, Fischli W: Effects of cilazapril, a novel angiotensin converting enzyme inhibitor, on the structure of pulmonary arteries of rats exposed to chronic hypoxia. J Cardiovasc Pharmacol 1991, 17(1):36-40.
2. Diller GP, Gatzoulis MA: Pulmonary vascular disease in adults with congenital heart disease. Circulation 2007, 115(8):1039-1050.
3. GNU General Public License, unspecified. http://www.gnu.org/copyleft/gpl.html
4. Heeneman S, Sluimer JC, Daemen MJ: Angiotensin-converting enzyme and vascular remodeling. Circ Res 2007, 101(5):441-454.
5. Herget J, Pelouch V, Kolar F, Ostadal B: The inhibition of angiotensin converting enzyme attenuates the effects of chronic hypoxia on pulmonary blood vessels in the rat. Physiol Res 1996, 45(3):221-226.

6. Hislop A, Reid L: New findings in pulmonary arteries of rats with hypoxia-induced pulmonary hypertension. Br J Exp Pathol 1976, 57(568):542-554.
7. Holmquist B, Bunning P, Riordan JF: A continuous spectrophotometric assay for angiotensin converting enzyme. Anal Biochem 1979, 95(2):540-548.
8. Hopkins N, McLoughlin P: The structural basis of pulmonary hypertension in chronic lung disease: remodelling, rarefaction or angiogenesis? J Anat 2002, 201(4):335-348.
9. Howell K, Preston RJ, McLoughlin P: Chronic hypoxia causes angiogenesis in addition to remodelling in the adult rat pulmonary circulation. J Physiol 2003, 547(Pt 1):133-145.
10. Humbert M, Morrell NW, Archer SL, Stenmark KR, MacLean MR, Lang IM, Christman BW, Weir EK, Eickelberg O, Voelkel NF, Rabinovitch M: Cellular and molecular pathobiology of pulmonary arterial hypertension. J Am Coll Cardiol 2004, 43(12 Suppl S):13S-24S.
11. Jeffery TK, Wanstall JC: Pulmonary vascular remodeling: a target for therapeutic intervention in pulmonary hypertension. Pharmacol Ther 2001, 92(1):1-20.
12. Jeffery TK, Wanstall JC: Pulmonary vascular remodelling in hypoxic rats: effects of amlodipine, alone and with perindopril. Eur J Pharmacol 2001, 416(1-2):123-131.
13. Jeffery TK, Wanstall JC: Perindopril, an angiotensin converting enzyme inhibitor, in pulmonary hypertensive rats: comparative effects on pulmonary vascular structure and function. Br J Pharmacol 1999, 128(7):1407-1418.
14. Karau KL, Johnson RH, Molthen RC, Dhyani AH, Haworth ST, Hanger CC, Roerig DL, Dawson CA: Microfocal X-ray CT imaging and pulmonary arterial distensibility in excised rat lungs. Am J Physiol Heart Circ Physiol 2001, 281(3):H1447-57
15. Leier CV, Bambach D, Nelson S, Hermiller JB, Huss P, Magorien RD, Unverferth DV: Captopril in primary pulmonary hypertension. Circulation 1983, 67(1):155-161.
16. Li M, Zhou TF, Liu HM, Hua YM, Wang XM: Effect of captopril on pulmonary vascular remodeling induced by left-to-right shunt in rats. Sichuan Da Xue Xue Bao Yi Xue Ban 2006, 37(2):242-245.
17. M.I.A. Lourakis. Levmar: Levenberg-Marquardt nonlinear least squares algorithms in C/C++. 2004. http://www.ics.forth.gr/~lourakis/levma/
18. Meyrick B, Reid L: The effect of continued hypoxia on rat pulmonary arterial circulation. An ultrastructural study. Lab Invest 1978, 38(2):188-200.
19. Molthen RC, Karau KL, Dawson CA: Quantitative models of the rat pulmonary arterial tree morphometry applied to hypoxia-induced arterial remodeling. J Appl Physiol 2004, 97(6):2372-84; discussion 2354.
20. Morrell NW, Atochina EN, Morris KG, Danilov SM, Stenmark KR: Angiotensin converting enzyme expression is increased in small pulmonary arteries of rats with hypoxia-induced pulmonary hypertension. J Clin Invest 1995, 96(4):1823-1833.
21. Morrell NW, Morris KG, Stenmark KR: Role of angiotensin-converting enzyme and angiotensin II in development of hypoxic pulmonary hypertension. Am J Physiol 1995, 269(4 Pt 2):H1186-94.
22. Nong Z, Stassen JM, Moons L, Collen D, Janssens S: Inhibition of tissue angiotensin-converting enzyme with quinapril reduces hypoxic pulmonary hypertension and pulmonary vascular remodeling. Circulation 1996, 94(8):1941-1947.
23. Rabinovitch M FAU - Gamble, W, Gamble W FAU - Nadas, A S, FAU NA, FAU MO, L R: Rat pulmonary circulation after chronic hypoxia: hemodynamic and structural features. (0002-9513):.
24. Rabinovitch M, Chesler N, Molthen RC: Point:Counterpoint: Chronic hypoxia-induced pulmonary hypertension does/does not lead to loss of pulmonary vasculature. J Appl Physiol 2007, 103(4):1449-1451.
25. Rabinovitch M, Haworth SG, Castaneda AR, Nadas AS, Reid LM: Lung biopsy in congenital heart disease: a morphometric approach to pulmonary vascular disease. Circulation 1978, 58(6):1107-1122.
26. Rakugi H, Kim DK, Krieger JE, Wang DS, Dzau VJ, Pratt RE: Induction of angiotensin converting enzyme in the neointima after vascular injury. Possible role in restenosis. J Clin Invest 1994, 93(1):339-346.
27. Robb RA, Hanson DP, Karwoski RA, Larson AG, Workman EL, Stacy MC: ANALYZE: A comprehensive, operator-interactive software package for multidimensional medical image display and analysis. Computerized Medical Imaging and Graphics 1989, 13:433-454.
28. Robb RA, Barillot C: Interactive display and analysis of 3-D medical Images. IEEE Transactions on Medical Imaging 1989, 8(3):217-226
29. Robb RA: The biomedical imaging resource at Mayo Clinic. IEEE Transactions on Medical Imaging 2001, 20(9):854-867

30. Shingrani R, Krenz G, Molthen R: Automation process for morphometric analysis of volumetric CT data from pulmonary vasculature in rats. Comput Methods Programs Biomed 2009, .
31. Smith K, Marshall JM: Physiological adjustments and arteriolar remodelling within skeletal muscle during acclimation to chronic hypoxia in the rat. J Physiol 1999, 521 Pt 1:261-272.
32. Steinhorn RH, Fineman JR: The pathophysiology of pulmonary hypertension in congenital heart disease. Artif Organs 1999, 23(11):970-974.
33. Tulloh RM: Congenital heart disease in relation to pulmonary hypertension in paediatric practice. Paediatr Respir Rev 2005, 6(3):174-180.
34. van Suylen RJ, Aartsen WM, Smits JF, Daemen MJ: Dissociation of pulmonary vascular remodeling and right ventricular pressure in tissue angiotensin-converting enzyme-deficient mice under conditions of chronic alveolar hypoxia. Am J Respir Crit Care Med 2001, 163(5):1241-1245.
35. Wang CG, Hakim TS, Michel RP, Chang HK: Segmental pulmonary vascular resistance in progressive hydrostatic and permeability edema. J Appl Physiol 1985, 59(1):242-247.